

https://doi.org/10.1070/QEL16953

On the issue of neutron source development for a laser-driven nuclear-thermonuclear reactor

G.V. Dolgoleva, I.G. Lebo

Abstract. **We discuss the feasibility of developing a high-power thermonuclear neutron source driven by laser pulses. Using one-dimensional numerical simulations for targets made in the form of double-sided cones, for an absorbed Nd-laser energy of ~1 MJ (at the second and third harmonics) and pulse duration of 10–20 ns it is possible to achieve a neutron yield at a level of 10^{16}–10^{17} per shot. This neutron yield is a prerequisite to the commencement of work to develop a hybrid nuclear-thermonuclear reactor.**

Keywords: *neutron source, conic target, numerical simulations.*

1. Introduction

Laser fusion (LF) research has been pursued in our country and abroad since the 60s of the past century [1]. It is planned to control the chain fission reactions in nuclear-thermonuclear reactors by initiating a series of microexplosions and generating high-power fluxes of thermonuclear neutrons (see, for instance, Ref. [2]). To pass from research work (the first stage) to the development (the second stage) of such reactors calls for the production of a LF-based neutron source with a thermonuclear neutron yield of at least 10^{16} per shot for a laser energy input of ~1 MJ. To state in different terms, this calls for the achievement of a target energy gain G of 0.1–1 ($G = E_{\rm fus}/E_{\rm las}$, where $E_{\rm fus}$ is the thermonuclear energy released in a microexplosion and $E_{\rm las}$ is the energy of a laser pulse absorbed in the target). Several significant requirements are imposed on the laser (driver), namely: the operation at a pulse repetition frequency of 1–10 Hz, an efficiency of the order of 10% or higher, the stability of producing pulses of designated energy, a long service life without a general overhaul, and economic justifiability [3, 4].

Constructed in the USA was a high-power neodymium glass laser, National Ignition Facility (NIF), with a pulse energy of ~2 MJ and a pulse duration of 10–20 ns, which is used to carry out research in the initiation of thermonuclear microexplosions [5]. Similar lasers are under construction in our country [6] and other leading countries of the world (in France and People's Republic of China). A neutron yield of the order of 10^{16} per pulse has been attained on the NIF facility by indirect irradiation (the energy of a laser pulse is converted to X-rays with the subsequent heating and compression of the working thermonuclear target) [7]. This is still insufficient for making the driver in a nuclear-thermonuclear reactor (since the neodymium laser does not meet other requirements listed above). However, the 'physical thermonuclear reaction threshold' was demonstrated on the NIF, when the energy released in the fusion reactions became equal to the energy inputted into the fuel by extraneous sources*.

The 'indirect irradiation' mode is not the optimal one in the development of a thermonuclear neutron source (driver) for future nuclear-thermonuclear reactors due to a large loss in energy conversion, the complexity of realising a stable neutron yield, and several other factors [8]. The feasibility of using conic targets for these purposes was discussed in Refs [8–12]. In this configuration, it is extremely difficult to obtain high densities of the DT mixture simultaneously with its heating to thermonuclear temperatures because of the deformation of the cone walls by the shock wave produced in the compressed fuel. Consequently, there is no way of obtaining a high energy gain in the target. To achieve $G \approx 1$, it would suffice to compress the fuel to a density of the order of 10 g cm^{-3} (i.e. to the normal density of gold or natural uranium, which the cone walls can be made of). The authors of Refs [8, 12] came up with the idea of producing a counterpressure in the wall near the vertex of two counter-cones with the use of a series of ultrashort superhigh-power laser pulses. This would make it possible to realise the 'dynamic confinement' of the plasma for a period of ~1 ns, during which the bulk of thermonuclear energy release would take place.

The proposed design is favoured by the following fact. In the majority of experiments in the compression of spherical shell targets with a laser pulse, an agreement between the simulated and experimental data on the neutron yield is observed for a volume compression of up to 10^3. Then there occurs a significant lowering of the thermonuclear reaction rate in comparison with the predictions of one-dimensional simulations. The reason is as follows: after a strong reflected shock wave reaches the shell, there occurs a rapid growth of hydrodynamic instability in it and the shell material mixes with the fuel.

An additional factor that leads to a lowering of the neutron yield is the displacement of the central part of the target due to asymmetric shell irradiation resulting from the transfer

G.V. Dolgoleva M.V. Lomonosov Moscow State University, Faculty of Mechanics and Mathematics, Vorob'evy Gory, 119991 Moscow, Russia; e-mail: dolgg@list.ru;
I.G. Lebo Moscow Technological University (MIREA), Institute of Cybernetics, prosp. Vernadskogo 78, 119454 Moscow, Russia; e-mail: lebo@mirea.ru

Received 26 January 2019; revision received 7 March 2019
Kvantovaya Elektronika **49** (8) 796–800 (2019)
Translated by E.N. Ragozin

*We note that about ~10% of the total energy deposited into the plasma finds its way to the fuel. Therefore, attaining $G \approx 1$ calls for a neutron yield of at least 3×10^{17} per shot for an absorbed laser energy of 1 MJ.

of directional momentum to the plasma [13, 14, 15]*. It is quite difficult to position the target precisely at the focus of a hundred of laser beams at a distance of the order of several metres (the radius of reactor chamber). This is technically simple to achieve with the help of a cylindrical target with conic channels inside, for instance, by imparting rotational motion to the target, like with a bullet in a barrel.

The development of a driver for a hybrid reactor invites a large investment and a thorough scientific and technical work. An experiment on the NIF or the UFL-2M facility under construction might be the first step in this direction [6]. To this end, even today there is good reason to provide for the corresponding configuration of light beams in the facility, the possibility to simultaneously generate long and short laser pulses, diagnostic techniques, and the corresponding design of the target chamber.

In the present paper we set forth the results of our numerical simulations of the neutron yield, which were made with the SND code [16, 17] for double-sided target cones under irradiation conditions corresponding to the NIF and UFL-2M facilities.

2. Brief description of the physicomathematical model of the SND programme

The one-dimensional Lagrangian method was developed for calculating the targets for thermonuclear (laser and heavy-ion) fusion. At its foundation is the system of equation of nonequilibrium radiative gas dynamics, which comprises gas dynamic equations (with the inclusion of electron and ion temperatures) and the heat transfer by ions and electrons with diffusion flux limitation. The SND programme provides for the possibility to calculate the radiative transfer in the quasi-diffusion approximation and the radiation–matter interaction, the absorption and transfer of laser energy, the kinetics of thermonuclear reactions, and the ionisation kinetics for taking into account the nonstationary behaviour of the medium. The atomic ionisation kinetics was calculated in the average ion approximation [16].

Below we set forth the system of equations without the inclusion of plasma radiation transfer:

$$
\begin{aligned}
&\frac{\mathrm{d}v}{\mathrm{d}t} = -\, r^{\theta}\frac{\partial(p_{\mathrm{e}} + p_{\mathrm{i}} + \mu)}{\partial m},\\
&\frac{\mathrm{d}}{\mathrm{d}t}\left(\frac{1}{\rho}\right) = \frac{\partial}{\partial m}(r^{\theta}v),\\
&\frac{\mathrm{d}r}{\mathrm{d}t} = v,\\
&\frac{\mathrm{d}\varepsilon_{\mathrm{e}}}{\mathrm{d}t} = -\, p_{\mathrm{e}}\frac{\partial}{\partial m}(r^{\theta}u) - \frac{\partial W_{\mathrm{e}}}{\partial m} + \frac{\partial q}{\partial m} + Q_{\mathrm{ke}} + Q_{\mathrm{ie}} + \dot{E}_{\alpha\mathrm{e}},\\
&\frac{\mathrm{d}\varepsilon_{\mathrm{i}}}{\mathrm{d}t} = -\,(p_{\mathrm{i}} + \mu)\frac{\partial}{\partial m}(r^{\theta}u) - \frac{\partial W_{\mathrm{i}}}{\partial m} + Q_{\mathrm{ki}} - Q_{\mathrm{ie}} + \dot{E}_{\alpha\mathrm{i}},\\
&W_{\mathrm{e,i}} = \min\left(-\chi_{\mathrm{e,i}} r^{\theta}\frac{\partial T_{\mathrm{e,i}}}{\partial r}, S_{\mathrm{max\,e,i}}\right).
\end{aligned}
\qquad (1)
$$

Also solved are the equations of the thermonuclear kinetics for tritium, deuterium, and helium-3. The transfer of α-particles was calculated in the multigroup diffusion approximation. Parameter θ in Eqns (1) is the index of symmetry ($\theta = 2$ – spherical, $\theta = 1$ – cylindrical, $\theta = 0$ – plane symmetry);

$$m = \int_0^r r^{\theta}\rho\,\mathrm{d}r$$

is the Lagrangian symmetry; r is the Eulerian radius; $\varepsilon_{\mathrm{e,i}}$, $p_{\mathrm{e,i}}$ and $T_{\mathrm{e,i}}$ are the internal energy, the pressure, and the temperatures of electrons and ions, respectively; v is the velocity; ρ is the density; q is the laser radiation flux; μ is the mathematical viscosity; $S_{\mathrm{max\,e,i}}$ are the electron and ion heat flux limits, respectively; χ_{e} and χ_{i} are the electron and ion heat transfer coefficients; Q_{ke}, Q_{ki} are the thermonuclear particle energies deposited into the electron and ion plasma components; $\dot{E}_{\alpha}$ is the power transferred from thermonuclear charged particles to the plasma; and Q_{ie} is the energy exchange between the electron and ion components.

In this paper we did not study the X-ray radiative transfer in the plasma. The simulations were performed using the simplified version of the SND programme [see Eqns (1)].

The methods for the solution of the above physicomathematical model and a comparison with the results of simulations of laser-driven spherical shell target compression performed by other methods are described in Refs [17, 18].

3. Problem formulations and results of numerical simulations

Figure 1 is a schematic representation of a double-sided conic target and its irradiation by laser beams borrowed from Refs [8, 12]. In our simulations, the cone walls were assumed to be perfectly elastic and thermally impermeable. The formation of a shell–wall boundary layer was neglected. The problem is perfectly symmetric about the truncated cone vertex (the symmetry plane, which is perpendicular to the axis O_1O_2, passes through the axis O_3O_4 shown in Fig. 1). The compression and thermonuclear reaction initiation in this target may be con-

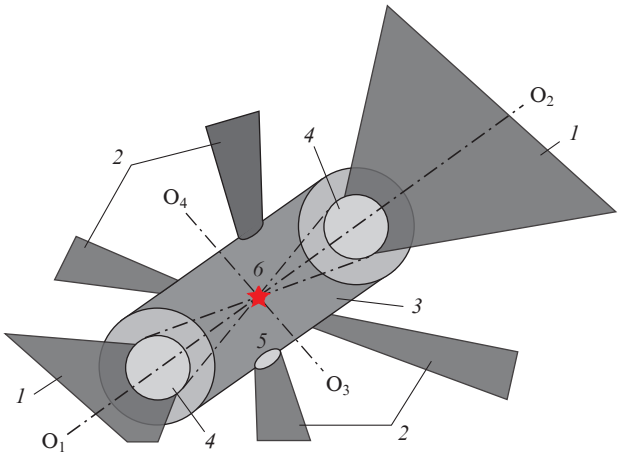

Figure 1. Schematic representation of the double-sided conic target and its irradiation by long and short laser pulses:
(O_1O_2) symmetry axis; (*1*) liner-accelerating laser beams (long pulses); (*2*) short laser pulses; (*3*) cylindrical target with counter conic channels along the axis O_1O_2; (*4*) shell liner; (*5*) openings for the injection of short pulses; (*6*) thermonuclear microexplosion; (O_3O_4) axis passing through the target centre in the plane perpendicular to the symmetry axis O_1O_2.

*As is noteworthy, an approximately 50-μm displacement of the compressed target core was discovered in experiments performed on the Delfin Facility, which corresponds to the predictions of numerical simulations (see Ref. [14], p. 106, Fig. 4.8c).

ventionally divided into two stages. At the first stage, a long laser pulse accelerates the liner, which moves towards the cone vertex and compresses the DT fuel. When the shock wave reaches the truncated cone vertex and is reflected, a sequence of short pulses (total duration: about 1 ns; total energy: 5%–10% of the main heating pulse [12]) is introduced into the target through the openings in the plane perpendicular to the O_1O_2 axis. The purpose of these pulses is to provide dynamic confinement of the compressed fuel and its additional heating (the second stage).

The time dependence of a laser pulse

$$\dot{E}(t) = \dot{E}_0 \begin{cases} \left(\frac{t}{t_1}\right)^2, \text{if } t < t_1, \\ 1, \text{if } t_1 < t < t_2, \\ \frac{t_3 - t}{t_3 - t_2}, \text{if } t_2 < t < t_3, \end{cases} \qquad (2)$$

$$\dot{E}_0 = E_{las} / \left(\frac{t_3 + t_2}{2} - \frac{2}{3} t_1 \right)$$

is plotted in Fig. 2. The parameters were borrowed from Ref. [18], but the pulse duration $t_3 = 21$ ns, which corresponds to the low foot mode, which was realised in experiments at the NIF (see, for instance, Ref. [8]).

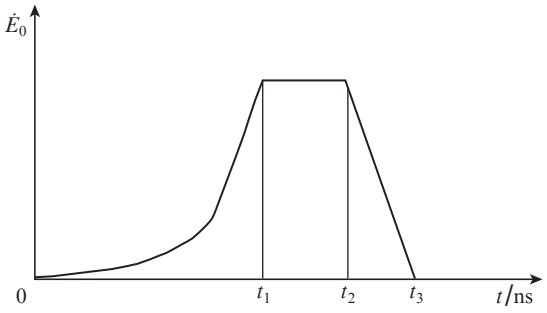

Figure 2. Temporal shape of a laser pulse; $t_1 = 12$ ns, $t_2 = 20$ ns, and $t_3 = 21$ ns.

The first stage involving acceleration to the centre and compression of the target described above was simulated with the help of the one-dimensional SND programme in spherical geometry. The laser pulse energy E_{las} calculated for the entire sphere (i.e. in a solid angle of 4π) was equal to 20.5 MJ; The radiation wavelength λ was equal to 0.35 μm. Hence, the energy per one cone with a solid angle $\Delta\Omega = 0.306$ sr (which corresponds to a cone vertex angle $\alpha = 0.627$ rad, or $\sim 36°$) was equal to 0.5 MJ. We assumed that 100% of laser energy was absorbed by the plasma. The radiative energy transfer from the heated plasma was neglected.

In the first series of simulations we considered a target of simplified design – a spherical CH-polymer shell filled with DT gas. In the selection of optimal gas-filled target parameters we proceeded from the scheme proposed in Ref. [14]. The heart of this scheme is as follows: relatively crude simulations are preliminarily made of thin shell targets for selecting the shell mass in such a way as to make its compression time equal to the pulse duration. This target mass is referred to as matched to the laser pulse. We then fix this mass and successively vary its thickness, initial radius, and the DT gas density ρ_0 to maximise the neutron yield.

Figure 3a displays the 'section' of the gas-filled target: the minimal radius R_{min}, the inner shell radius R_0, and the shell thickness Δ_{CH}. To maximise the neutron yield prior to the shell disruption due to hydrodynamic instability development, we selected the ratio $R_0/R_{min} \approx 10$ (i.e. the volume compression by no more than 1000 times).

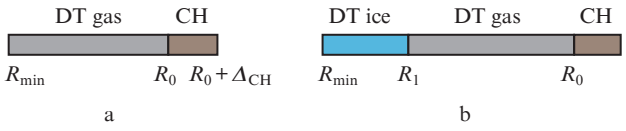

Figure 3. (a) Gas-filled and (b) cryogenic target structures.

We varied the CH layer thickness (the initial density: 1 g cm^{-3}; atomic ion mass $A = 6.5$; average ion charge $Z = 3.5$), R_{min}, and the initial DT gas density ρ_0. Based on the one-dimensional numerical simulations, we selected the following parameters: $R_0 = 0.5–0.505$ cm, $\Delta_{CH} = 90$ μm, and $\rho_0 = 0.23$ mg cm^{-3}. The shell may freely expand at the outer shell–vacuum boundary. A perfectly elastic heat-insulated wall was assumed to be at the $r = R_{min}$ boundary.

The best results for two series of simulations for $R_{min} = 0.05$ cm, $R_0 = 0.5$ and 0.505 cm are collected in Table 1. One can see that $G_{max} \approx 0.03$ for $R_{min} = 0.05$ cm. The neutron yield is easily calculated: $Y_n = (3.55 \times 10^{17})G$ neutrons for an energy of 1 MJ inputted into the plasma. Therefore, with the gas-filled target it is possible to attain $Y_n \approx 10^{16}$. To increase the neutron yield for a fixed laser energy, it is necessary to go over to cryogenic targets or provide additional fuel compression owing to short laser pulses and a complex target structure.

Table 1.

R_0	t_{col}/ns	r_{col}/cm	Gain G	DT mass in 4π/g	Liner thickness Δ_{CH}/μm
0.5	20.55	0.051	0.03	1.208E-4	90
0.505	20.7	0.0512	0.032	1.208E-4	90

Note: t_{col} is the instant of greatest compression and r_{col} is the radius of DT mixture at the point in time t_{col}.

In the third series of simulations we analysed a cryogenic target, when a spherical condensed DT ice (or liquid) layer of thickness $R_1 - R_{min}$ was placed at the vertex inside of the spherical target. The DT vapour density in the gap between the condensed fuel and the shell was equal to 10^{-5} g cm^{-3}, $R_{min} = 0.05$ cm. The shell thickness Δ_{CH}, R_1, and R_0 were varied in the simulations. The laser wavelength $\lambda = 0.35$ μm. The target masses were matched to the laser pulse. Table 2 lists the best results of the third series for 90- and 85-μm thick shells.

Table 2.

R_1	t_{col}/ns	r_{col}/cm	Gain G	DT mass in 4π/g	Liner thickness Δ_{CH}/μm
0.12	20.55	0.0542	0.3138	1.684E-3	90
0.12	20.05	0.0547	0.267	1.684E-3	85

It is easily calculated that a double-sided conic target with a solid angle $\Delta\Omega = 0.306$ sr irradiated by a 1-MJ laser pulse

provides a neutron yield $Y_n \approx 10^{17}$. In this series, the CH-shell aspect ratio was also $R_0/\Delta_{CH} \approx 56-59$.

In the next (fourth) series of simulations we simulated the compression of the double-sided conic target using the second Nd-laser harmonic, i.e. at a wavelength $\lambda = 0.53$ μm. The time characteristics of the laser pulse were the same as in the previous series. The ratio $R_0/R_{min} = 10.1$ remained practically as before. The results of numerical simulations are collected in Table 3.

Table 3.

R_1	t_{col}/ns	r_{col}/cm	Gain G	Liner thickness Δ_{CH}/μm
0.12	21.5	0.054	0.19	90
0.12	20.9	0.0543	0.18	85

We note that increasing the shell aspect ratio $R_0/\Delta_{CH} \approx 59$ did not result in a significant change in G. Going over from the third to the second harmonic of neodymium laser radiation resulted in an insignificant lowering of the neutron yield. The reason is as follows: unlike small experimental shells, where the radiation is absorbed primarily in the vicinity of the critical plasma density, in reactor-scale targets the absorption of laser radiation is distributed over the corona*.

The efficiency of laser radiation conversion to the second harmonic might be expected to increase in comparison with the conversion to the third harmonic, and this would supposedly increase the net efficiency of the thermonuclear source.

4. Conclusions

We have studied the liner acceleration by a laser pulse and the compression of DT fuel under the assumption of 'dynamic plasma confinement'. The possibilities of a stable liner flight, its interaction with the wall of a conic channel, and, lastly, the organisation of dynamic confinement of compressed DT fuel with the help of a series of short laser pulses have not been simulated. The authors of Ref. [12] proposed a target design (Fig. 4a), which made use of a low-density coating, an aerogel, to achieve uniform heating and symmetrise ablation pressure (see also Ref. [19]).

Figure 4b shows the domain near the vertex of the counter cones. Located between the gold wall and the gold foil is a low-density aerogel – a 'foam' of lower density than the critical plasma density for the corresponding laser wavelength. This foam, like in the former case, is intended to absorb short laser pulses and equalise the plasma pressure on the inner wall (the gold foil), which confines the DT fuel [20, 21]. It is well to bear in mind that an important role at the stage of deceleration and thermonuclear reaction 'burst' will be played radiative and thermonuclear particle transfer, which must be included in the description of this stage.

Simulating the compressed DT fuel domain calls for the development of a three-dimensional gas-kinetic code to numerically solve plasmadynamics equations simultaneously with the equations of energy transfer by suprathermal electron fluxes. Such codes are inaccessible to us for the present. However, in our next paper we plan to study the effect of radiative and thermonuclear particle energy transfer in the compression region of the conic target in the framework of one-dimensional geometry.

An additional complication is the simulation of a porous medium, in which there are thin walls of density 1 g cm^{-3} and a low-density gas. The problem of energy transfer in this medium was studied earlier (see, for instance, Refs [22–30]). However, developing the general physicomathematical model for the interaction of high-power laser pulses with low-density porous media and for the energy transfer in this medium, in our opinion, invites further experimental and numerical research.

*This work does not consider SBS, self-focusing, and other effects which may turn out to be significant in lengthy plasma coronas of reactor targets.

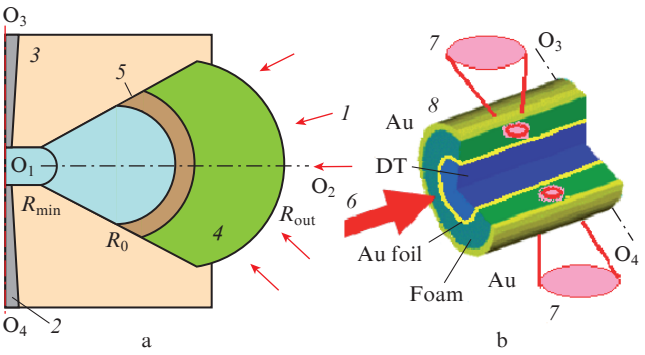

Figure 4. Structure of (a) half the conic target (the outer part) and (b) the target near the cone vertex:
(O_1O_2) axis of the truncated counter cones; (O_3O_4) axis located in the symmetry plane, which is perpendicular to O_1O_2; (*1*) laser beams of the first (long) pulse; (*2*) openings for injecting short laser pulses; (*3*) conic target walls; (*4*) low-density foam-like absorber; (*5*) liner; (*6*) direction of liner's motion under long-pulse irradiation; (*7*) short laser pulses injected into the target through the openings and absorbed by the aerogel; (*8*) thick cone wall.

References

1. Basov N.G., Krokhin O.N. *JETP*, **19** (1), 123 (1964) [*Zh. Eksp. Teor. Fiz.*, **46** (1), 171 (1964)].
2. Basov N.G., Subbotin V.I., Feoktistov L.P. *Vestn. Ross. Akad. Nauk*, **63** (10), 878 (1993).
3. Basov N.G., Belousov N.I., Vergunova G.A., et al. *Sov. J. Quantum Electron.*, **15** (3), 380 (1985) [*Kvantovaya Elektron.*, **12** (3), 584 (1985)].
4. Basov N.G., Lebo I.G., Rozanov V.B. *Fizika lazernogo termoyadernogo sinteza* (Physics of Laser Thermonuclear Fusion) (Moscow: Znanie, 1988).
5. Moses E.I. et al. *Nuclear Fusion*, **53**, 104020 (2013).
6. Garanin S.G., Bel'kov S.A., Bondarenko S.V. *XXXIX Mezhdunarodnaya (Zvenigorodskaya) Konf. po Fizike Plazmy i UTS* (XXXIX Intern. (Zvenigorod) Conf. on Plazma Phys. and Controlled Thermonuclear Fusion) (Zvenigorod, 2012) p.17.
7. Le Pape S., Berzak Hopkins L.F., Divol L., et al. *Phys. Rev. Lett*, **120**, 245003 (2018).
8. Kuzenov V.V., Lebo A.I., Lebo I.G., Ryzhkov S.V. *Fizikomatematicheskie modeli i metody rascheta vozdeistviya moshchnykh lazernykh i plazmennykh impul'sov na kondensirivannye i gazovye sredy* (Physicomathematical Models and Methods of Simulation of the Action of High-Power Laser and Plasma Pulses on Condensed and Gas Media) (Moscow: Izd-vo MGTU im. N.E. Baumana, 2015).
9. Basov N.G., Lebo I.G., Rozanov V.B., Tishkin V.F., Feoktistov L.P. *Quantum Electron.*, **28** (4), 316 (1998) [*Kvantovaya Elektron.*, **25** (4), 327 (1998)].
10. Lebo I.G. *Quantum Electron.*, **30** (5), 409 (2000) [*Kvantovaya Elektron.*, **30** (5), 409 (2000)].

11. Krasyuk I.K., Semenov A.Yu., Charakhch'yan A.A. *Quantum Electron.*, **35** (9), 769 (2005) [*Kvantovaya Elektron.*, **35** (9), 769 (2005)].
12. Lebo I.G., Isaev E.A., Lebo A.I. *Quantum Electron.*, **47** (2), 106 (2017) [*Kvantovaya Elektron.*, **47** (2), 106 (2017)].
13. Gamalii E.G., Demchenko N.N., Lebo I.G., et al. *Sov. J. Quantum Electron.*, **18** (8), 1012 (1988) [*Kvantovaya Elektron.*, **15** (8), 1622 (1988)].
14. Lebo I.G., Tishkin V.F. *Issledovaniya gidrodinamicheskoi neustoichivosti v zadachakh lazernogo termoyadernogo sinteza* (Investigation of Hydrodynamic Instability in Laser Thermonuclear Fusion Problems) (Moscow: FIZMATLIT, 2006).
15. Bel'kov S.A., Bondarenko S.V., Vergunova G.A., et al. *JETP*, **124** (2), 341 (2017) [*Zh. Eksp. Teor. Fiz.*, **151** (2), 396 (2017)].
16. Bel'kov S.A., Dolgoleva G.V. *VANT. Ser. Metod. i Progr. Chisl. Resheniya Zadach Matem. Fiz.*, (1), 59 (1992).
17. Dolgoleva G.V. *VANT. Ser. Metod. i Progr. Chisl. Resheniya Zadach Matem. Fiz.*, (2), 29 (1983).
18. Dolgoleva G.V., Lebo A.I., Lebo I.G. *Matem. Model.*, **238** (1), 23 (2016).
19. Lebo I.G., Rozanov V.B., Tishkin V.F. *Laser Part. Beam.*, **12** (3), 361 (1994).
20. Lebo I.G., Popov I.V., Rozanov V.B., Tishkin V.F. *Quantum Electron.*, **25** (12), 1220 (1995) [*Kvantovaya Elektron.*, **22** (12), 1257 (1995)].
21. Rozanov V.B. *Phys. Usp.*, **47** (4), 359 (2004) [*Usp. Fiz. Nauk*, **174** (4), 371 (2004)].
22. Afshar-rad T., Desselberger M., Dunne M., et al. *Phys. Rev. Lett.*, **73** (1), 74 (1994).
23. Dune M., Borghesi M., Ivase A., et al. *Phys. Rev. Lett.*, **75** (21), 3858 (1995).
24. Bugrov A.E., Burdonskii I.N., Gavrilov V.V., et al. *JETP*, **88** (3), 441 (1999) [*Zh. Eksp. Teor. Fiz.*, **115** (3), 805 (1999)].
25. Borisenko N.G., Akunets A.A., Khalenkov A.M., et al. *J. Russ. Laser Res.*, **28** (6), 548 (2007).
26. Borisenko N.G., Merkuliev Yu.A. *J. Russ. Laser Res.*, **31** (3), 256 (2010).
27. Lebo A.I., Lebo I.G. *Matem. Model.*, **21** (1), 75 (2009).
28. Lebo A.I., Lebo I.G. *Matem. Model.*, **21** (11), 16 (2009).
29. Lebo I.G., Lebo A.I. *Vestnik MGTU MIREA*, (3), 215 (2014).
30. Rozanov V.B., Barishpol'tsev D.V., Vergunova G.A., et al. *JETP*, **122** (2), 256 (2016) [*Zh. Eksp. Teor. Fiz.*, **149** (2), 294 (2016)].